

Dileptons from bremsstrahlung: going beyond the soft photon approximation¹

H.C. Eggers

Department of Physics, University of Stellenbosch, 7600 Stellenbosch, South Africa

C. Gale¹, R. Tabti¹, and K. Haglin²

¹*Department of Physics, McGill University, Montréal QC, Canada H3A 2T8*

²*National Superconducting Cyclotron Laboratory, Michigan State University
East Lansing, MI 48824-1321, USA*

The traditional calculation of dilepton yields from bremsstrahlung relies on the assumption that electromagnetic and strong processes factorize. We argue that this assumption, embodied by the soft photon approximation, cannot hold true for invariant mass spectra on very general grounds. Deriving a formula for the dilepton cross section for pion-pion scattering that does not rely on such factorization, we formulate the problem exactly in terms of three-particle phase space invariants. Using a simple one boson exchange model for comparison, we find that dilepton cross sections and yields are generally overestimated by the soft photon approximation by factors 2–8. In extreme cases, overestimation up to a factor 40 is possible.

1 Introduction

Interest in the use of dileptons as a probe of the hot and early phases of heavy ion collisions is fed by the desire of finding new physics such as the vaunted quark gluon plasma and generally probing the behavior of nuclear matter under extreme conditions [1]. Recent data by HELIOS and NA38 [2] and discrepancies found by CERES [3] have provided impetus to hopes that new physics is finally in sight. Realising such hopes, however, requires detailed understanding of background processes: the contribution from each must be calculated quantitatively.

While quantitative calculations are challenging already on a technical level, it is a much harder problem to identify untested assumptions that enter such calculations and to quantify their effects. We here aim to show, by example of bremsstrahlung from pion-pion scattering, that the “soft photon approximation” (SPA) represents such an untested assumption [4].

¹ To be published in *International Conference on Structure of Vacuum and Elementary Matter*, Wilderness, South Africa, March 10–16, 1996 (World Scientific).

2 Why the SPA must fail

Conventional dilepton yields at very low invariant masses $M < 500$ MeV are dominated by Dalitz decays and bremsstrahlung. Calculations of such bremsstrahlung yields rely heavily on the soft photon approximation because it is simple to use. This simplicity is achieved mainly through the assumption that the electromagnetic and strong processes factorize.

In order for this assumption to be valid, two conditions [5] must be met: First, the photon energy q_0 must be much smaller than the energy E_i of any one of the hadrons participating in the scattering, $q_0/E_i \ll 1$; secondly, the hadronic and electromagnetic scales must be sufficiently different to permit separate treatment. This translates into the condition $q_0 \ll m_Y |\mathbf{p}_i|/E_i$, where m_Y is the mass of the exchange boson. For the case where two hadrons of equal mass m collide, these equations read in their cms

$$q_0 \ll \sqrt{s}/2, \quad (1)$$

$$q_0 \ll m_Y \sqrt{1 - 4m^2/s}. \quad (2)$$

Implicit in these equations is, of course, a specific Lorentz frame with respect to which the energies are measured. In a simple bremsstrahlung experiment, these limits are easily satisfied by selecting only photons or dileptons of low energy in the laboratory frame. In the complex multiparticle systems formed in the course of nucleus-nucleus collisions, however, there are many binary collisions, and their respective cms frames do not generally coincide either with one another or with the overall nucleus-nucleus cms frame.

In such a situation, it is better to look at relativistically invariant quantities, such as the dilepton invariant mass M . Looking at invariant masses means that q_0 is no longer fixed but must vary over its full kinematic range, which for our example of colliding equal-mass hadrons is given by

$$M \leq q_0 \leq \frac{s - 4m^2 + M^2}{2\sqrt{s}}. \quad (3)$$

In Figure 1, we show the three functions (1) and (2) and (3) for the case $m = m_\pi = 140$ MeV, $m_Y = m_\sigma \simeq 500$ MeV and dilepton invariant masses $M = 10$ and 300 MeV. It is immediately clear that the assumptions underlying the SPA are not fulfilled even for small M : the kinematic range accessible to q_0 is never much smaller than the limits set by the SPA. The situation becomes even worse for larger M .

3 Cross sections: approximate and exact

In order to quantify what effect the use of the SPA has on yields, it is necessary to compare approximate cross sections to an exact formulation. All such dilepton cross sections can be written [6] as the product of a purely leptonic prefactor

$$\kappa \equiv (\alpha/3\pi) \left[1 + (2\mu^2/M^2) \right] \sqrt{1 - 4\mu^2/M^2}$$

(with μ the lepton rest mass) times the cross section for production of a virtual photon γ^* with mass M ,

$$d\sigma_{hh\ell^+\ell^-} = \kappa d\sigma_{hh\gamma^*}. \quad (4)$$

Now the traditional procedure has been to factorise the virtual photon cross section $d\sigma_{hh\gamma^*}$ into electromagnetic and strong pieces, writing it in terms of a current J^μ and three-particle phase space

$$dR_3 \equiv \delta^4(p_a + p_b - p_1 - p_2 - q)(d^3p_1/2E_1)(d^3p_2/2E_2)(d^3q/2q_0),$$

$$d\sigma_{hh\gamma^*} = 4\pi\alpha \frac{dM^2}{M^2} (-J^\mu J_\mu) |\mathcal{M}_h|^2 \frac{dR_3}{(2\pi)^5 F}, \quad (5)$$

where F is the incoming flux. It turns out that such factorization is unnecessary. A re-derivation yields exactly, without factorization [4],

$$d\sigma_{hh\gamma^*} = \frac{dM^2}{M^2} \left[-\sum_{mn} (\mathcal{M}_m)^\mu (\mathcal{M}_n^*)_\mu \right] \frac{dR_3}{(2\pi)^5 F}, \quad (6)$$

where m, n run over all diagrams of the reaction $\pi\pi \rightarrow \pi\pi\gamma^*$, including emission by the central blob.

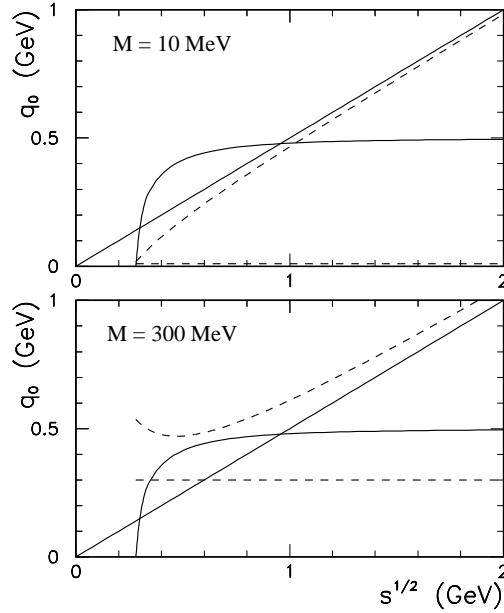


Figure 1: The region between the dashed lines is the domain of integration for q_0 when calculating cross sections as a function of dilepton invariant mass. The SPA is valid only when q_0 is much smaller than the two solid lines shown. This is clearly not the case.

Since people do not like 3-particle phase space, dR_3 is usually simplified by neglecting q in the delta function, permitting reduction to 2-phase space $dR_3 \simeq dR_2 (d^3q/2q_0)$, with $dR_2 \equiv \delta(p_a + p_b - p_1 - p_2)(d^3p_1/2E_1)(d^3p_2/2E_2)$. Eqs. (4), (5) then simplify to the Rückl form [7, 8]

$$\frac{d\sigma_{hh\ell^+\ell^-}^{\text{Rückl}}}{dM^2} = \frac{3}{2} \frac{\kappa}{M^2} \frac{\alpha}{\pi} \int d\sigma_{hh} \int_M^A dq_0 \sqrt{q_0^2 - M^2} \int \frac{d\Omega_q}{4\pi} (-J^\mu J_\mu), \quad (7)$$

where $d\sigma_{hh}$ is the on-shell cross section for the purely hadronic reaction $\pi\pi \rightarrow \pi\pi$. The current is first angle-averaged over the photon solid angle $d\Omega_q$ and then integrated over

the kinematic range $M \leq q_0 \leq A = [s + M^2 - 4m^2]/2\sqrt{s}$ of the photon energy q_0 . At this point an ad hoc factor to correct for the factorization of dR_3 is usually also included.

A better derivation by Lichard [6] led to a form similar to Eq. (7) but without the $(3/2)$ prefactor and with the inclusion of q and M in the current.

In order to use the exact formulation (6), by contrast, it is necessary to formulate $d\sigma_{hh\gamma^*}$ in terms of *three-particle phase space* invariants, which for the schematic reaction $a + b \rightarrow 1 + 2 + 3$ are defined [9] as $s = (p_a + p_b)^2$, $t_1 = (p_1 - p_a)^2$, $s_1 = (p_1 + p_2)^2$, $s_2 = (p_2 + p_3)^2$, and $t_2 = (p_b - p_3)^2$. The final-state phase space integral is then given by [9]

$$dR_3(s) = \frac{\pi}{4\lambda^{1/2}(s, m_a^2, m_b^2)} \int \frac{dt_1 ds_2 ds_1 dt_2}{\sqrt{B}}, \quad (8)$$

weighted by the 6×6 Cayley determinant B and where $\lambda(x, y, z) = (x - y - z)^2 - 4yz$. One then obtains exactly

$$\frac{d\sigma_{hh\ell^+\ell^-}^{\text{exact}}}{dM^2} = \frac{4\pi\alpha}{(2\pi)^5 M^2} \frac{\kappa(M^2)\pi}{8\lambda(s, m_a^2, m_b^2)} \int \frac{dt_1 ds_2 ds_1 dt_2}{\sqrt{B}} \left[-\sum_{mn} (\mathcal{M}_m)^\mu (\mathcal{M}_n^*)_\mu \right], \quad (9)$$

where all terms $(\mathcal{M}_m)^\mu (\mathcal{M}_n^*)_\mu$ are written in terms of the five invariants.

As a by-product of the 3-particle phase space language, one can define an intermediate approximation which, while still factorising the electromagnetic part out of $d\sigma_{hh\ell^+\ell^-}$, writes the current J in terms of its invariants [4]:

$$\begin{aligned} \frac{d\sigma_{hh\ell^+\ell^-}}{dM^2} &\simeq \frac{4\pi\alpha}{(2\pi)^5 M^2} \frac{\kappa\pi}{8\lambda(s, m_a^2, m_b^2)} \int dt_1 |\mathcal{M}_h(s, t_1)|^2 \\ &\times \int \frac{ds_2 ds_1 dt_2}{\sqrt{B}} \left[-J^2(s, t_1, s_2, s_1, t_2) \right]. \end{aligned} \quad (10)$$

4 One boson exchange model

Equation (9) may be exact in terms of the matrix elements \mathcal{M} , but it does not specify what \mathcal{M} should be. For a quantitative comparison of the approximations (7) and (10) to the exact cross section (9), we must therefore turn to a simple microscopic model of pion-pion interactions [4]. We use a simple one boson exchange model with the σ , ρ and $f(1270)$ mesons included. The hadronic part of the lagrangian

$$\mathcal{L} = g_\sigma \sigma \partial_\mu \pi \cdot \partial^\mu \pi + g_\rho \rho^\mu \cdot \pi \times \partial_\mu \pi + g_f f_{\mu\nu} \partial^\mu \pi \cdot \partial^\nu \pi \quad (11)$$

is fitted to elastic $\pi^+\pi^-$ collision data to fix the constants, then supplemented through minimal substitution by the corresponding electromagnetic interaction lagrangian. We work at tree level only. Monopole strong form factors are included for t and u -channels; no electromagnetic form factors are needed at present. Virtual photon emission is implemented gauge-invariantly for pion and ρ emission as well as the $\pi\pi\sigma$, $\pi\pi f$ and $\pi\pi\rho$ vertices.

This model is probably far from a perfect description of the pion-pion interaction, so that results obtained below can serve merely as a good pointer towards answering the question: How different are the results when we use the SPA or the exact cross section?

5 Numerical results

To quantify the differences between the approximations and the exact formulation, we have studied the five distinct pion-pion reactions. Writing $(+-) \rightarrow (+-)$ as shorthand for the reaction $(\pi^+\pi^- \rightarrow \pi^+\pi^-\ell^+\ell^-)$ and so on, we have calculated within our OBE model cross sections for $(+-) \rightarrow (+-)$, $(++) \rightarrow (++)$, $(+-) \rightarrow (00)$, $(00) \rightarrow (+-)$ and $(+0) \rightarrow (+0)$. Numerical results were checked by performing a number of consistency checks, including testing for gauge invariance in the σ , ρ and f sectors separately.

Figures 2–4 show the cross sections $d\sigma_{hh\ell+\ell-}$ for dielectron production from the five distinct reactions as functions of \sqrt{s} , for $M = 10$ MeV and 300 MeV respectively. Final-state symmetrization factors were included where appropriate. Initial-state symmetrization was also included for $(++) \rightarrow (++)$ and $(00) \rightarrow (+-)$ in order to facilitate use within a thermal pion gas environment. Because they are identical in structure to their charge-conjugate versions, cross sections for the reactions $(+0) \rightarrow (+0)$ and $(++) \rightarrow (++)$ were doubled. All cross sections were computed using the same OBE model and parameter values.

We see that there is a complete hodgepodge of curves, with a few underestimating the “exact” cross sections (solid lines) but most overestimating the exact curves by factors 1–5. The largest discrepancy between approximations and the exact result occur for the reaction $(++) \rightarrow (++)$ (Figure 4): for the Rückl approximation, factors 3 (for 10 MeV) to 40 (for 300 MeV) arise, while the Lichard approximation yields corresponding overestimation factors of 1.9 and 14–20.

In Figure 5, we attempt to cast some light on the physical origin of the discrepancies observed. Plotted are the cross sections for reactions $(++) \rightarrow (++)$ and $(+-) \rightarrow (00)$. The upper lines correspond, as before, to the Rückl, Lichard and 3-phase space current approximations, while the solid line again represents the exact result. The lowest dash-dotted line, on the other hand, represents the exact result but excluding all internal ² diagrams and their cross terms with external ones. The difference between this lower line and the exact result (solid line) therefore represents the contribution of the internal diagrams; while the difference between the lower dash-dotted line and the upper lines (approximations) represents the change in cross section due to inclusion/exclusion of q in the *external*-emission diagrams. We see that the contribution of internal emission is not all that large, albeit nonnegligible. By far the most important effect on $d\sigma/dM$ is the neglect of the dependence of \mathcal{M} on the photon momentum q . We believe that this neglect is at the heart of the considerable differences between approximations and exact results.

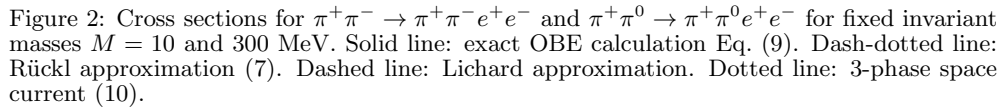
Finally, Figure 6 shows the dilepton production rates per unit spacetime summed over all seven reactions, calculated using the Boltzmann formula [10]

$$\frac{dN_{\ell+\ell-}^{\text{Boltz}}}{d^4x dM^2} = \frac{1}{32\pi^4} \int ds \lambda(s, m^2, m^2) \frac{K_1(\sqrt{s}/T)}{(\sqrt{s}/T)} \frac{d\sigma_{hh\ell+\ell-}}{dM^2} \quad (12)$$

for temperatures $T = 100$ and 200 MeV respectively. Right-hand panels show the corresponding ratios, obtained by dividing a given approximate by the “exact” result. Again,

² “Internal” diagrams are those for which the photon is emitted at a hadronic vertex or by the exchange boson.

Note that none of the approximations approaches the exact result for small values of M : even for the smallest value shown ($M = 10$ MeV), the discrepancy is still above 40% for the Lichard and current approximations and larger than a factor 2 for the Rückl approximation.



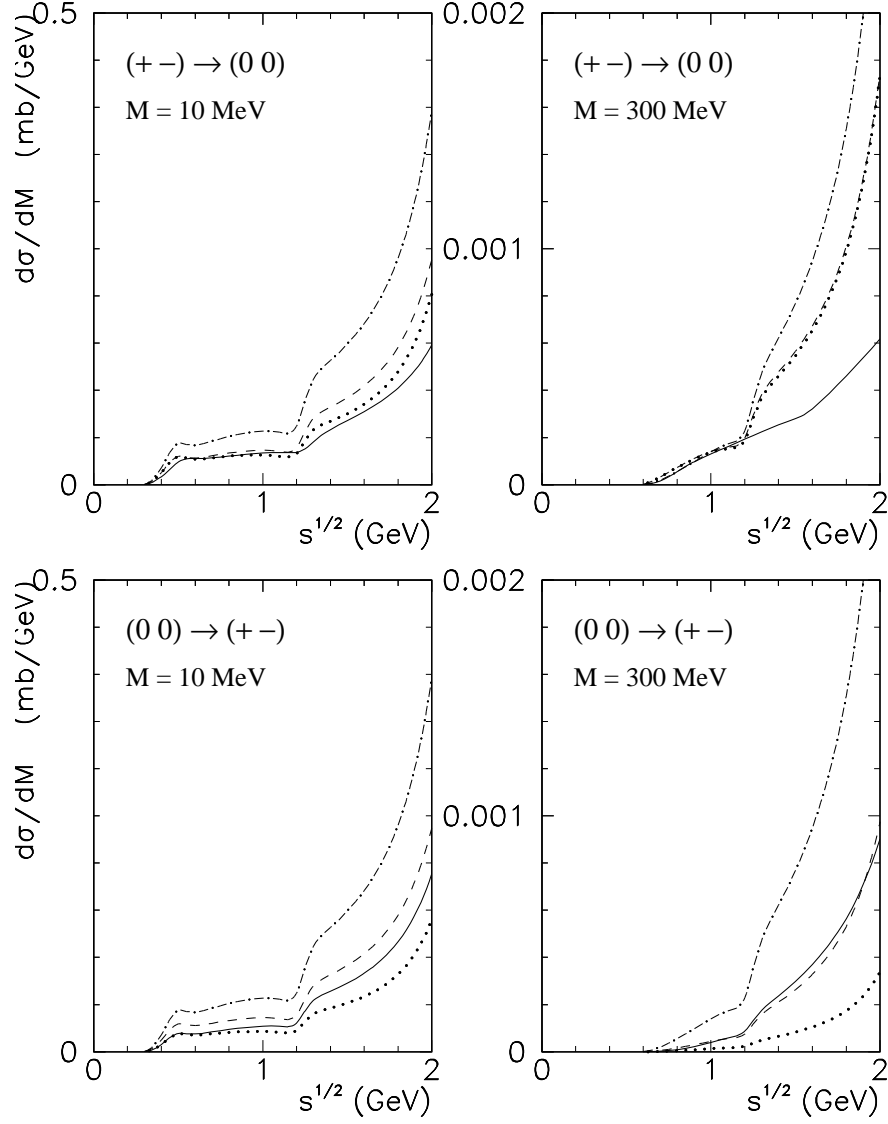


Figure 3: Same as Figure 2, for the reactions $\pi^+\pi^- \rightarrow \pi^0\pi^0 e^+e^-$ and $\pi^0\pi^0 \rightarrow \pi^+\pi^- e^+e^-$.

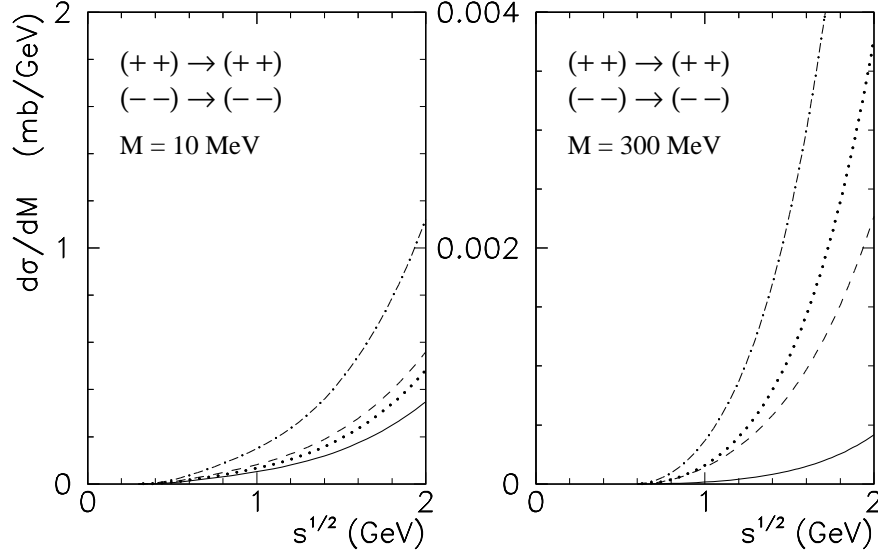


Figure 4: Same as Figure 2, for the reaction $\pi^+\pi^+ \rightarrow \pi^+\pi^+e^+e^-$.

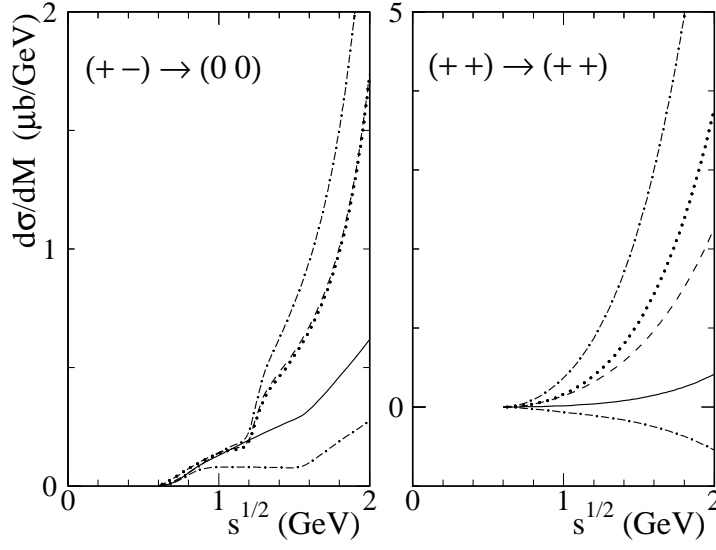


Figure 5: Contribution of external-emission vs. external-plus-internal diagrams for the reactions $(+-) \rightarrow (00)$ and $(++) \rightarrow (++)$ for $M = 300$ MeV. Lines are as in Figs. 3 and 4. The new dash-dotted line below the (solid line) exact calculation represents contributions arising solely from emission of γ^* by an external pion line, but taking q into account in \mathcal{M} , in contrast to the approximations (upper lines) which neglected q .

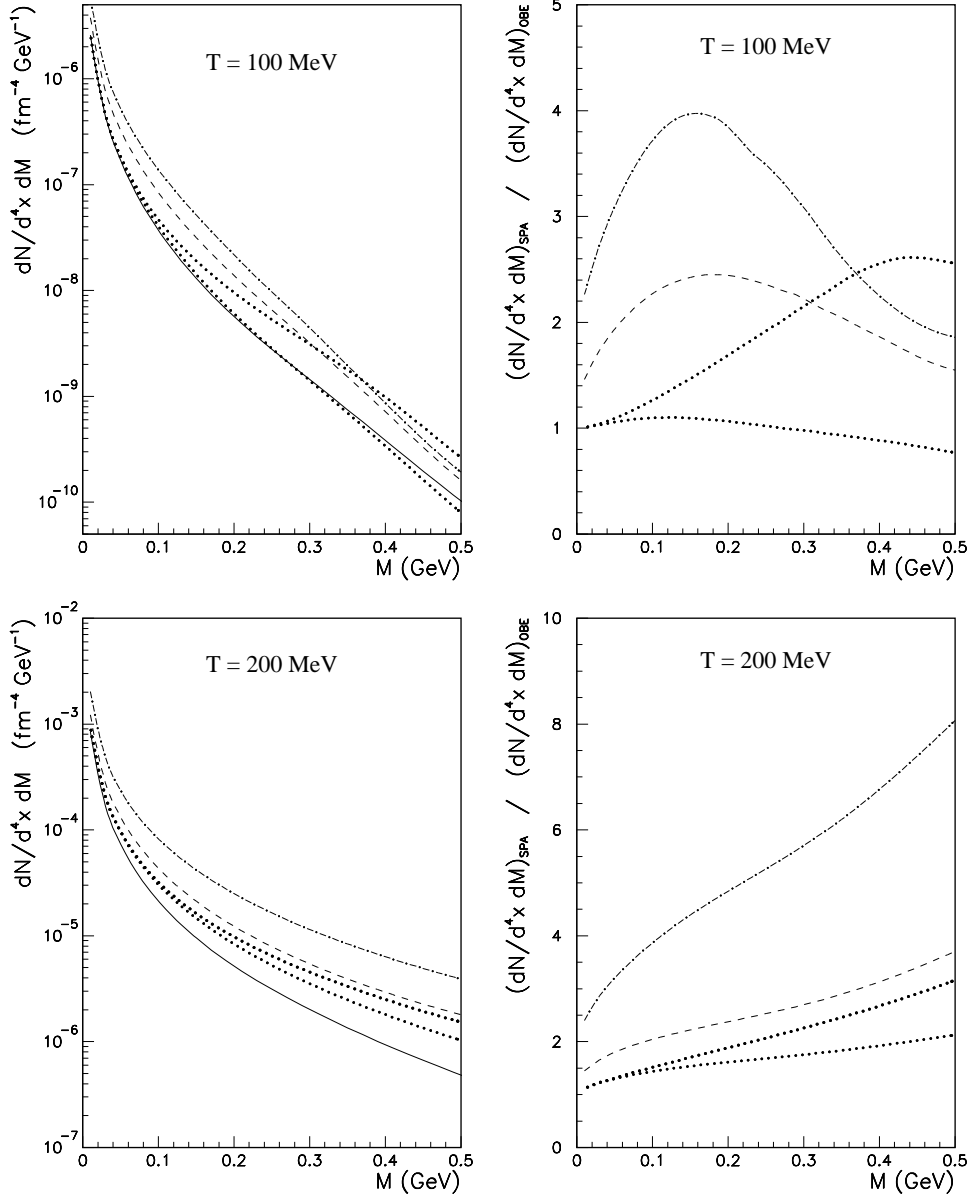


Figure 6: Left: Total bremsstrahlung yields of e^+e^- for all seven pion-pion reactions, for a Boltzmann gas with temperatures $T = 100 \text{ MeV}$ and $T = 200 \text{ MeV}$. Right: Ratios of SPA approximation calculations divided by exact OBE rate. Solid line: exact OBE calculation, Dash-dotted line: Rückl approximation, Dashed line: Lichard approximation, Dotted line: 3-phase space current, including (upper) and excluding (lower) the mass of the virtual γ^* in the current.

We hence believe that the SPA is flawed when used in a heavy ion context except in special situations. The suppression of the “exact” rates compared to traditional calculations shown here would imply that bremsstrahlung dielectrons cannot make up for the discrepancies between measured dielectron rates and the cocktail of reactions used for comparison. Greater attention will have to be paid to the $\pi\pi$ annihilation, η Dalitz and other channels contributing at low M . The suppression we find would also have a bearing on calculations of the Landau-Pomeranchuk effect [11].

Acknowledgments

This work was supported in part by the Austrian Fonds zur Förderung der wissenschaftlichen Forschung (FWF), the Natural Sciences and Engineering Research Council of Canada, the Québec FCAR fund, a NATO Collaborative Research Grant, and the National Science Foundation.

References

- [1] J.W. Harris and B. Müller, *The Search for the Quark-Gluon Plasma*, hep-ph/9602235, to appear in *Ann. Rev. Nucl. Part. Sci.*.
- [2] HELIOS-3 Collaboration, T. Åkesson et al., *Z. Phys. C* **68**, 47 (1995); NA38 Collaboration, C. Lourenco et al., in *Proc. 11th Int. Conf. on Ultrarelativistic Nucleus-Nucleus Collisions*, Monterey, Jan. 9–13, 1995, *Nucl. Phys. A* **590**, 1c (1995).
- [3] NA45/CERES Collaboration, G. Agakichiev et al., *Phys. Rev. Lett.* **75**, 1272 (1995).
- [4] H.C. Eggers, R. Tabti, C. Gale and K. Haglin, hep-ph/9510409, *Phys. Rev. D* **53**, 4822 (1996).
- [5] F. Low, *Phys. Rev.* **110**, 974 (1958).
- [6] P. Lichard, *Phys. Rev. D* **51**, 6017 (1995).
- [7] R. Rückl, *Phys. Lett. B* **64**, 39 (1976).
- [8] K. Haglin, C. Gale and V. Emel’yanov, *Phys. Rev. D* **47**, 973 (1993).
- [9] E. Byckling and K. Kajantie, *Particle Kinematics*, (Wiley, London, 1973).
- [10] K. Kajantie, J. Kapusta, L. McLerran and A. Mekjian, *Phys. Rev. D* **34**, 2746 (1986).
- [11] J. Cleymans, V.V. Goloviznin and K. Redlich, *Phys. Rev. D* **47**, 989 (1993).